Optica Applicata, Vol. LII, No. 4, 2022
DOI: 10.37190/oa220413

Properties of an electromagnetic twisted Gaussian Schell-model array beam propagating in anisotropic atmosphere turbulence

Xianyang Yang[1,*], Wenyu Fu[2,3,**], Xuehua Hu[2], Xue Li[2]

[1] School of Intelligent Manufacturing and Energy Engineering, Jiang-Xi University of Engineering, Xinyu, 33800, Jiangxi, China

[2] College of Science, Jiang-Xi University of Engineering, Xinyu, 33800, Jiangxi, China

[3] Department of Physics, Long Dong University, Qingyang, Gansu, 745000, China

*Corresponding author: yangxy2013@hotmail.com

**Corresponding author: qytcfwy@163.com

The effect of anisotropic atmosphere turbulence on propagation characteristics of an electromagnetic twisted Gaussian Schell-model array (EM TGSMA) beam is investigated. An analytical expression for the cross-spectral density function of such beam propagating through anisotropic turbulent atmosphere is derived and used to explore the evolutionary behavior of the spectral intensity, degree of polarization (DOP) and degree of coherence (DOC). An example illustrates the fact that twisted strength and anisotropic turbulent factors have an important impact on the behavior of spectral density, DOC and DOP, in particular. The rotation angle of the array beams can also be controlled by adjusting twisted strength. Furthermore, strong anisotropic turbulence was also found to cause significant mergence of the array beams. Our results might be beneficial for free-space communications of the partially coherent beams endowed with twist.

Keywords: partially coherent, array beams, twist phase, anisotropic atmosphere turbulence, propagation properties.

1. Introduction

Since Simon and Mukunda introduced a twist phase concept and imparted such phase to a Gaussian Schell model (GSM) beam [1], the GSM beam due to its potential applications has been widely investigated. A twist phase differs from the customary quadratic phase factor in many aspects. It exists only in partially coherent beams [1,2] and has an intrinsic chiral or handedness property. Thus, a beam with twist phase has orbital angular momentum and it induces a rotation of beam spots on propagation [3–5]. The recent results showed that orbital angular momentum of electromagnetic Gaussian Schell-model (EGSM) beam with twist phase closely depends on its twisted strength and degree of polarization in the source plane [6]. In Ref. [7], experimental observation of the twisted Gaussian Schell-model (TGSM) beam was reported. Since then, a variety of theoretical models and experimental schemes have been proposed to create new beams with twisted phrase [8–11]. It has been confirmed that the twisted phase play an important role in optical imaging, optical trapping and optical communications [12–14].

In order to realize the further utilization of laser beams in the fields of remote sensing, imaging and wireless information transmission [15–17], it is necessary to investigate the propagation characteristics of laser beams in random medium such as turbulent atmosphere and ocean. These researches contain the spectral changes, intensity and coherent properties of stochastic light beams [18–20], scintillation of various beams types [21,22], the bit error rate (BER) evaluations [23,24], the spreading and propagation factor of partially coherent beams [25,26], *etc*. Besides, the latest findings about stratospheric turbulence showed that atmosphere turbulence will also be anisotropic due to the earth's rotation [27–30]. It is well known that, in anisotropic turbulence, the physical parameters behave differently compared to the behavior in isotropic turbulence. Thus, it also becomes a particularly good topic to explore properties of laser beams propagating in anisotropic atmosphere turbulence.

On the other hand, the array distribution field deserves also more attention of researchers due to the wide applications in multiple fields including holographic optical tweezers [31], particles trapping [32], phonic lithography [33,34], *etc*. Compared with the single beam, the source size of coherent array beams diverges less, and can produce higher output power and lattice-like intensity distribution [35]. Recently, WAN and ZHAO presented a new kind of array beam with twist phase termed as twisted Gaussian Schell -model array (TGSMA) sources [36], whose spectral density and spectral degree of coherence can gradually rotate along its propagation direction. The properties of an electromagnetic twisted Gaussian Schell-model array (EM TGSMA) beam in free space were discussed [37]. However, the properties of the EM TGSMA beam propagating through anisotropic atmosphere turbulence have not been reported yet.

In this paper, we focus on changes of an EM TGSMA beam through anisotropic atmosphere turbulence. An analytical expression for describing the cross-spectral density function of such beam propagating through turbulent atmosphere will be derived based on the extended Huygens–Fresnel integral. By means of the obtained theoretical results, the effect of the twisted strength and anisotropic atmosphere turbulence on the EM TGSMA beam will be studied in detail.

2. Description of the anisotropic atmosphere power spectrum

It is known that atmosphere turbulence will be anisotropic owing to the earth's rotation. To simplify the matter, the anisotropy of turbulence eddies is assumed to exist only in the propagation direction of the beam [38], and the horizontal extension of turbulence eddies is different from the vertical one. After considering anisotropy of atmospheric turbulence, anisotropic spectrum of atmosphere turbulence can be written as [30]

$$\varphi_n(\kappa) = \frac{0.033\, C_n^2 \mu_x \mu_y}{\left(\mu_x^2 \kappa_x^2 + \mu_y^2 \kappa_y^2 + \kappa_z^2\right)^{11/6}} \tag{1}$$

here C_n^2 is a generalized structure constant of the refractive-index with units m$^{-2/3}$. $\kappa = (\mu_x^2 \kappa_x^2 + \mu_y^2 \kappa_y^2 + \kappa_z^2)^{1/2}$ denotes the spatial frequency of atmosphere turbulent fluctuation along three orthogonal directions. And κ_z are spatial frequency components along three orthogonal directions in Markov approximation, κ_z (*i.e.* the z component of κ) can be ignored. μ_x and μ_y are the anisotropic factors along x- and y-direction, respectively. Without loss of generality, $\mu_x \neq \mu_y$, and thus, if propagation is in the z-direction, the orthogonal xoy-plane will no longer be circularly symmetric (*i.e.* isotropic). This may lead to different statistical values in the horizontal and vertical trans-

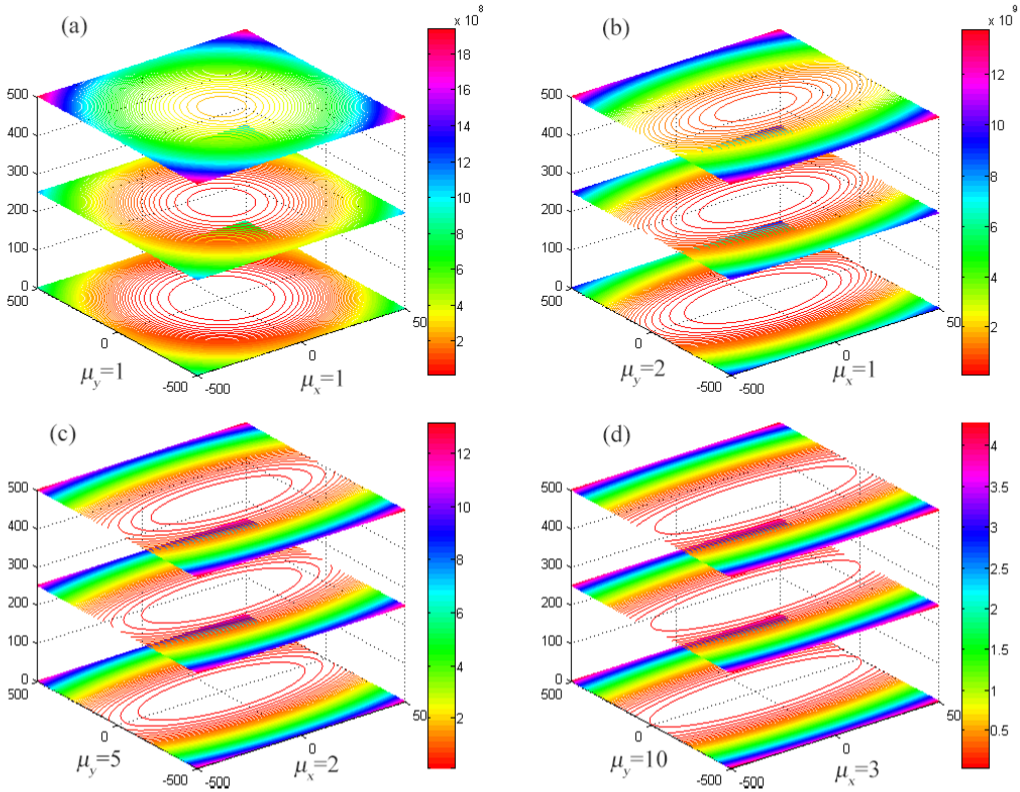

Fig. 1. Plot of the anisotropic spatial power spectrum $\varphi_n(\kappa)$ for several values of μ_x and μ_y. The color bar is the value of spacial power spectrum, the vertical and horizontal axes denote spacial frequency in three different directions, the units are m^{-1}.The turbulent structure constant $C_n^2 = 10^{-14}$ m$^{-2/3}$.

verse directions. However, for $\mu_x = \mu_y = 1$, Eq. (1) reduces to the conventional isotropic Kolmogorov spectrum. Because the spectrum is anisotropic we have to predict more accurately the behavior of turbulence when dealing with beam propagation. The calculated anisotropic spatial power spectra for different values of μ_x and μ_y are shown in Fig. 1. From Fig. 1(a)–(d), it can be seen that the anisotropic factors μ_x and μ_y have a very significant effect on distribution of spatial power spectrum. As anisotropic factors μ_x and μ_y increase, the spatial power spectrum intensity becomes larger, the spatial frequency scale of turbulent fluctuations increases, and the anisotropic effect of spatial power spectrum becomes more and more obvious.

3. Propagation of an EM TGSMA beam in anisotropic atmosphere turbulence

Based on the unified theory of coherence and polarization for a random partially coherent electromagnetic beam [39], in the Cartesian coordinate system, the element of cross-spectral density matrix (CSDM) of an EM TGSMA beam at source plane $z = 0$ can be expressed as [37]

$$W_{ij}(\mathbf{r}_1, \mathbf{r}_2) = \exp\left(-\frac{x_1^2 + x_2^2}{4\sigma_{1ij}^2}\right)\exp\left(-\frac{y_1^2 + y_2^2}{4\sigma_{2ij}^2}\right)\exp\left[-\frac{(x_1 - x_2)^2}{4\delta_{1ij}^2}\right]\exp\left[-\frac{(y_1 - y_2)^2}{4\delta_{2ij}^2}\right]$$
$$\times \sum_{n_1 = -P}^{P} \cos\left[C_{1ij}(x_1 - x_2)\right] \sum_{n_1 = -Q}^{Q} \cos\left[C_{2ij}(y_1 - y_2)\right]$$
$$\times \exp\left[-iu_{ij}x_1 y_2 + iu_{ij}x_2 y_1\right], \qquad (i, j = x, y) \tag{2}$$

where $\mathbf{r}_1 = (x_1, y_1)$ and $\mathbf{r}_2 = (x_2, y_2)$ are arbitrary two-dimensional position vectors; σ_{1ij} and σ_{2ij} denote the beams width, u_{ij} is the twisted strength, $P = (N_1 - 1)/2$ and $Q = (N_2 - 1)/2$, N_1 and N_2 are positive integrals which determine the number of array lobes; $C_{1ij} = 2\pi n_1 R_1/\delta_{1ij}$, $C_{2ij} = 2\pi n_2 R_2/\delta_{2ij}$, R_1, R_2, and δ_{1ij}, δ_{2ij} are coherence parameters. In the presence of a turbulence medium, employing the extended Huygens–Fresnel integral in the paraxial form, the element of CSDM of an EM TGSMA beam during propagation can be presented as following

$$W_{ij}(\rho_1, \rho_2, z) = \frac{k}{2\pi z}\iint W_{ij}(r_1, r_2)\exp\left[-ik\frac{(\rho_1 - r_1)^2 - (\rho_2 - r_2)^2}{2z}\right]$$
$$\times \langle \exp[\psi(\rho_1, r_1) + \psi^*(\rho_2, r_2)]\rangle_{\mathrm{R}} \mathrm{d}r_1 \mathrm{d}r_2 \tag{3}$$

where $k = 2\pi/\lambda$ denotes wave number, λ is the wavelength, ψ stands for the complex phase perturbation caused by the medium, $\langle\cdot\rangle_{\mathrm{R}}$ implies averaging over the ensemble of statistical realizations of the turbulence. Under quadratic phase approximations, $\langle\cdot\rangle_{\mathrm{R}}$ can be rewritten as

$$\begin{aligned}&\langle \exp[\psi(\rho_1, r_1) + \psi^*(\rho_2, r_2)]\rangle_{\mathrm{R}}\\ &\quad = \exp\left\{\frac{\pi^2 k^2 z}{3}\int_0^\infty \kappa^3 \varphi_n(\kappa)\mathrm{d}^3\kappa\left[(\rho_1-\rho_2)^2 + (\rho_1-\rho_2)(r_1-r_2) + (r_1-r_2)^2\right]\right\}\end{aligned} \tag{4}$$

where $\varphi_n(\kappa)$ is the spatial power spectrum of refractive-index fluctuation representing the anisotropic atmosphere characteristics. By substituting Eqs. (2) and (4) into Eq. (3) and performing mathematical calculation, we can obtain following expressions for each element of the cross-spectral density matrix of the EM TGSMA beam through anisotropic atmosphere turbulence

$$\begin{aligned}W_{ij}(\rho_1, \rho_2, z) &= \frac{\pi^2 E_{ij}}{16\lambda^2 z^2 \sigma_{1ij}\sqrt{a_{1ij} b_{ij} c_{ij} d_{ij}}}\exp\left[-\frac{ik(\rho_1^2-\rho_2^2)}{2z}\right]\\ &\quad\times\sum_{n_x=-P}^{P}\sum_{n_y=-Q}^{Q}(A+B+C+D)\end{aligned} \tag{5}$$

with

$$\begin{aligned}A &= \exp\left[\frac{X_{1ij+}^2}{a_{1ij}} + \frac{F_{ij+}^2}{b_{ij}} + \frac{1}{c_{ij}}\left(Y_{1ij+} - \frac{iu_{ij}}{2b_{ij}}F_{ij+}\right)^2\right.\\ &\quad\left. + \frac{1}{d_{ij}}\left(\gamma_{ij}X_{1ij+} - \eta_{ij}X_{2ij+} - \frac{m_{ij}}{2c_{ij}}Y_{1ij+} + Y_{2ij+}\right)^2\right]\end{aligned} \tag{6a}$$

$$\begin{aligned}B &= \exp\left[\frac{X_{1ij-}^2}{a_{1ij}} + \frac{F_{ij-}^2}{b_{ij}} + \frac{1}{c_{ij}}\left(Y_{1ij-} - \frac{iu_{ij}}{2b_{ij}}F_{ij-}\right)^2\right.\\ &\quad\left. + \frac{1}{d_{ij}}\left(\gamma_{ij}X_{1ij-} - \eta_{ij}X_{2ij-} - \frac{m_{ij}}{2c_{ij}}Y_{1ij-} + Y_{2ij-}\right)^2\right]\end{aligned} \tag{6b}$$

$$\begin{aligned}C &= \exp\left[\frac{X_{1ij+}^2}{a_{1ij}} + \frac{F_{ij+}^2}{b_{ij}} + \frac{1}{c_{ij}}\left(Y_{1ij-} - \frac{iu_{ij}}{2\,b_{ij}}F_{ij+}\right)^2\right.\\ &\quad\left. + \frac{1}{d_{ij}}\left(\gamma_{ij}X_{1ij+} - \eta_{ij}X_{2ij+} - \frac{m_{ij}}{2c_{ij}}Y_{1ij-} + Y_{2ij-}\right)^2\right]\end{aligned} \tag{6c}$$

$$D = \exp\left[\frac{X_{1ij-}^2}{a_{1ij}} + \frac{F_{ij-}^2}{b_{ij}} + \frac{1}{c_{ij}}\left(Y_{1ij+} - \frac{iu_{ij}}{2b_{ij}} F_{ij-}\right)^2 \right.$$
$$\left. + \frac{1}{d_{ij}}\left(\gamma_{ij} X_{1ij-} - \eta_{ij} X_{2ij-} - \frac{m_{ij}}{2c_{ij}} Y_{1ij+} + Y_{2ij+}\right)^2\right] \tag{6d}$$

and

$$E_{ij} = 1, \quad (i = j) \tag{6e}$$

$$E_{ij} = 0, \quad (i \neq j) \tag{6f}$$

$$X_{1ij\pm} = \frac{i}{2}\left(\frac{kx_1'}{z} \pm C_{1ij}\right) \tag{6g}$$

$$X_{2ij\pm} = \frac{i}{2}\left(\frac{kx_2'}{z} \pm C_{1ij}\right) \tag{6h}$$

$$Y_{1ij\pm} = \frac{i}{2}\left(\frac{ky_1'}{z} \pm C_{2ij}\right) \tag{6i}$$

$$Y_{2ij\pm} = \frac{i}{2}\left(\frac{ky_2'}{z} \pm C_{2ij}\right) \tag{6j}$$

$$F_{ij\pm} = X_{2ij\pm} - \frac{\xi_{1ij} X_{1ij\pm}}{a_{1ij}} \tag{6k}$$

$$M(z) = \frac{\pi^2 k^2 z}{3}\int_0^\infty \kappa^3 \varphi_n(\kappa)\mathrm{d}^3\kappa \tag{6l}$$

$$\xi_{1ij} = \frac{1}{\delta_{1ij}^2} - 2M(z) \tag{6m}$$

$$\xi_{2ij} = \frac{1}{\delta_{2ij}^2} - 2M(z) \tag{6n}$$

$$a_{1ij} = \frac{1}{4\sigma_{1ij}^2} + \frac{1}{2\delta_{1ij}^2} + \frac{ik}{2z} - M(z), \quad (i, j = x, y) \tag{6o}$$

$$a_{2ij} = \frac{1}{4\sigma_{2ij}^2} + \frac{1}{2\delta_{2ij}^2} - \frac{ik}{2z} - M(z), \quad (i, j = x, y) \tag{6p}$$

$$b_{ij} = a_{1ij}^* - \frac{\xi_{1ij}(z)}{4a_{1ij}} \tag{6q}$$

$$c_{ij} = \frac{1}{4\sigma_{2ij}^2} + \frac{1}{2\delta_{2ij}^2} + \frac{ik}{2z} + \frac{u_{ij}^2}{4b_{ij}} \tag{6r}$$

$$d_{ij} = a_{2ij}^* + \frac{u_{ij}^2}{4a_{1ij}} + \frac{u_{ij}^2 \xi_{1ij}^2}{16a_{1ij}b_{ij}} - \frac{m_{ij}^2}{4c_{ij}} \tag{6s}$$

$$\eta_{ij} = \frac{iu_{ij}}{4b_{ij}}\left(\frac{\xi_{1ij}}{a_{1ij}} - \frac{m_{ij}}{c_{ij}}\right) \tag{6t}$$

$$\gamma_{ij} = \frac{1}{2a_{1ij}}(iu_{ij} + \eta_{ij}\xi_{1ij}) \tag{6u}$$

$$m_{ij} = \xi_{2ij} + \frac{u_{ij}^2 \xi_{1ij}}{4a_{1ij}b_{ij}} \tag{6v}$$

Equations (5) and (6) can be considered as a general analytical expression of the CSDM for the EM TGSMA beam. For $N_1 = N_2 = 1$, it would reduce to the propagated CSDM for the EM TGSM beam. Using Eqs. (5) and (6), one can study the statistical properties of such EM TGSMA beam on propagation. Setting $\rho_1 = \rho_2 = \rho$, the average intensity for the EM TGSMA beam propagating in anisotropic atmosphere turbulence can be expressed as [19,20,37]

$$S(\rho, z) = W_{xx}(\rho, \rho, z) + W_{yy}(\rho, \rho, z) \tag{7}$$

the degree of polarization (DOP) of the beams with uncorrelated beams components can be calculated by the expression

$$P(\rho, z) = \frac{|W_{xx}(\rho, \rho, z) - W_{yy}(\rho, \rho, z)|}{W_{xx}(\rho, \rho, z) + W_{yy}(\rho, \rho, z)} \tag{8}$$

the degree of coherence (DOC) at a pair of points ρ_1 and ρ_2 generally is given by

$$\mu(\rho_1, \rho_2, z) = \frac{W(\rho_1, \rho_2, z)}{\sqrt{W(\rho_1, \rho_1, z)W(\rho_2, \rho_2, z)}} \tag{9}$$

4. Numerical results and discussions

In the this section, we choose the common laser with wavelength $\lambda = 0.632$ μm as an example to numerically examine the behavior of the EM TGSMA beam propagating in anisotropic atmosphere turbulence. The other global parameters used in the following calculations are set as $R_1 = 2R_2 = 3$ mm, $N_1 = 2$, $N_2 = 1$, unless it is specified in the figure captions. Firstly, we discuss the intensity behavior of the EM TGSMA beam.

Figure 2 illustrates the evolution of the spectral intensity of the EM TGSMA beam in the near field propagating through anisotropic atmosphere turbulence. Owing to the fact that the effect of turbulent medium on the array beams is relatively weaker, the behavior of the array beams depends on the initial Gaussian initial parameters. The initial Gaussian ellipse spots progressively split into an array and all lobes rotate around its center in a synchronous motion, and the rotating direction lies on twisted strengths of the array beams. With the increase of propagation distance, the intensity profiles transform from a horizontal ellipse to a vertical ellipse. Figure 3 shows the evolution of the spectral intensity of the EM TGSMA beam in the far field propagating through anisotropic atmosphere turbulence. It can be found that with the increase of propagation distance, the accumulative effect of anisotropic turbulence on the array beams becomes

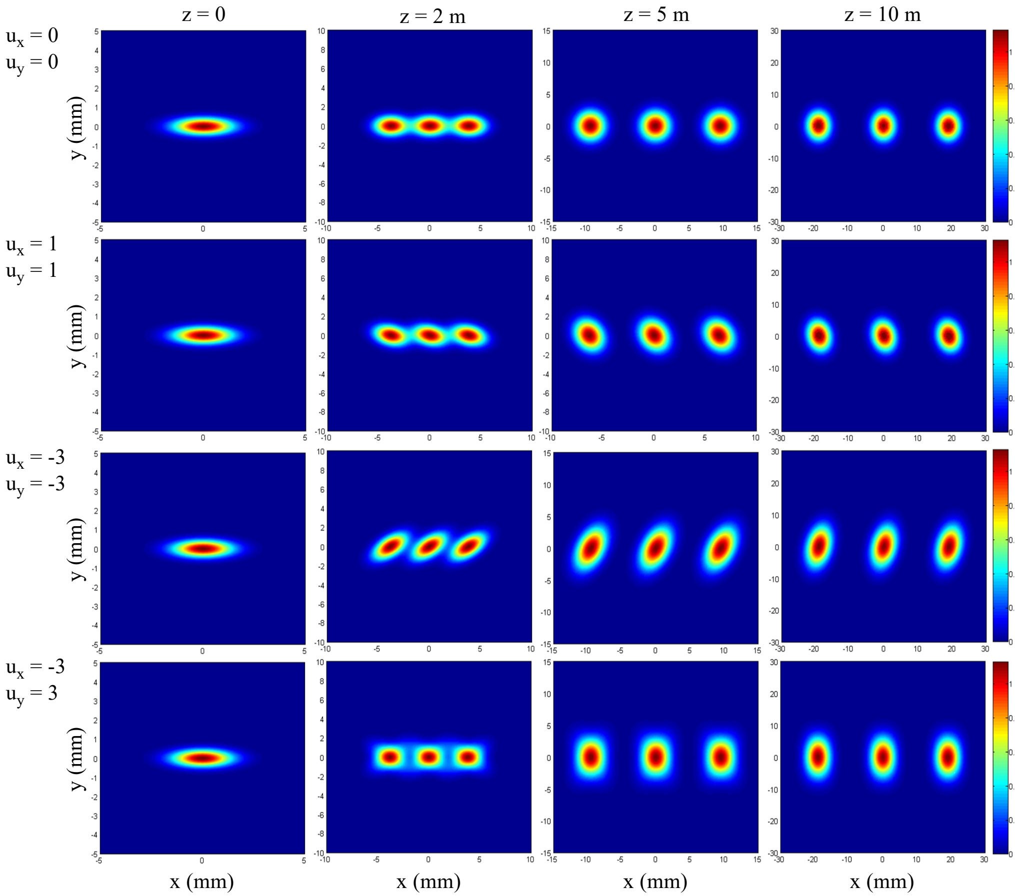

Fig. 2. The normalized intensity of the EM TGSMA beam in the near field propagating through anisotropic atmosphere turbulence for different values of twisted strengths. Beam parameters are chosen: $\sigma_{1xx} = \sigma_{1yy} = 1$ mm, $\sigma_{2xx} = \sigma_{2yy} = 0.3$ mm, $\delta_{1xx} = \delta_{1yy} = 0.5$ mm, and $\delta_{2xx} = \delta_{2yy} = 0.4$ mm, atmosphere turbulent parameters are chosen as $C_n^2 = 10^{-14}$ m$^{-2/3}$, $\mu_x = 2$, and $\mu_y = 5$.

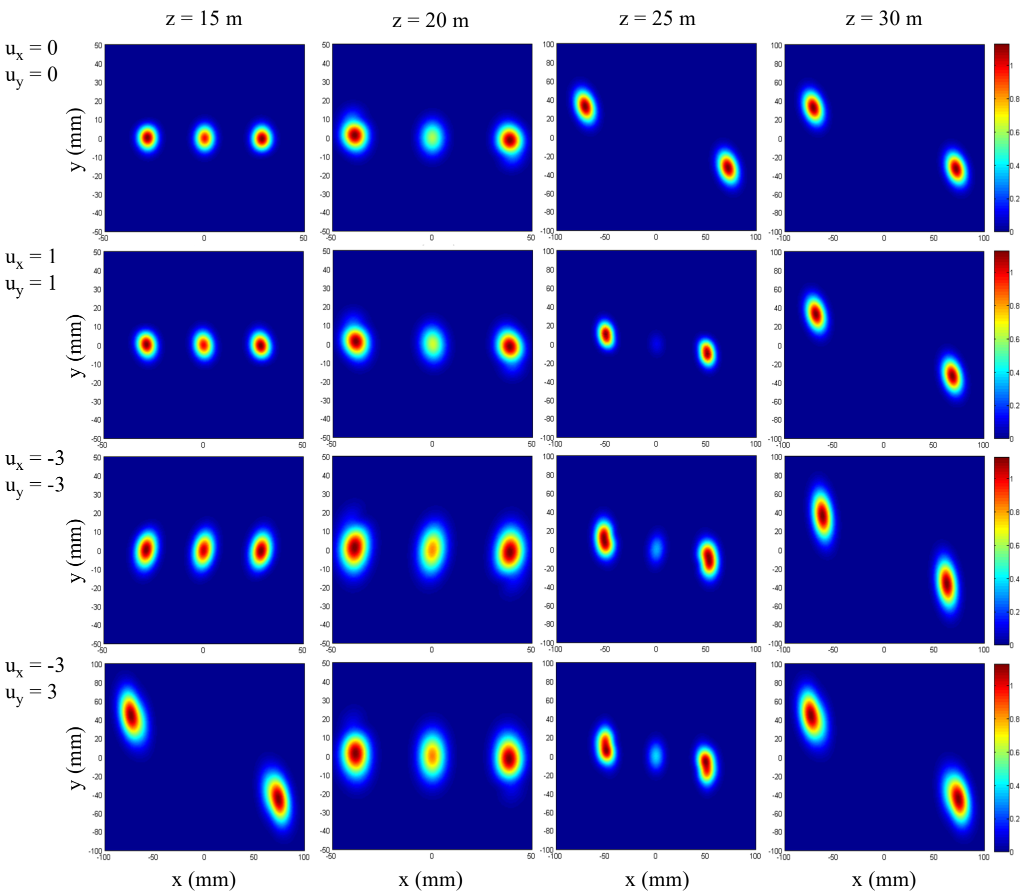

Fig. 3. The normalized intensity of the EM TGSMA beam in the far field propagating through anisotropic atmosphere turbulence for different values of twisted strengths. Beam parameters are same as those in Fig. 2.

gradually obvious, and mergence of the array beams occurs. The intensity of the two side-lobes increases while the intensity of the center-lobes decays rapidly, meanwhile the side-lobes not only revolve counter-clockwise by a certain angle but also move their positions as the propagation distance changes, and this means that the anisotropy of atmospheric turbulence plays a dominant role in determining the intensity and location of the side-lobes when the beam travels a sufficiently long distance. This novel results of the array beams in anisotropic atmospheric turbulence may provide a further insight into the EM TGSMA beam. In Fig. 4, we analyze numerically the evolution of the EM TGSMA beam in different conditions of the turbulence and twisted strengths. Figure 4(a) shows that a variety of rotation angle of the array beams *versus* propagation distance for different values of twisted strengths. It can be found from Fig. 4(a) that the rotation angle of the array beams monotonically raises from 0° to 90° and the ro-

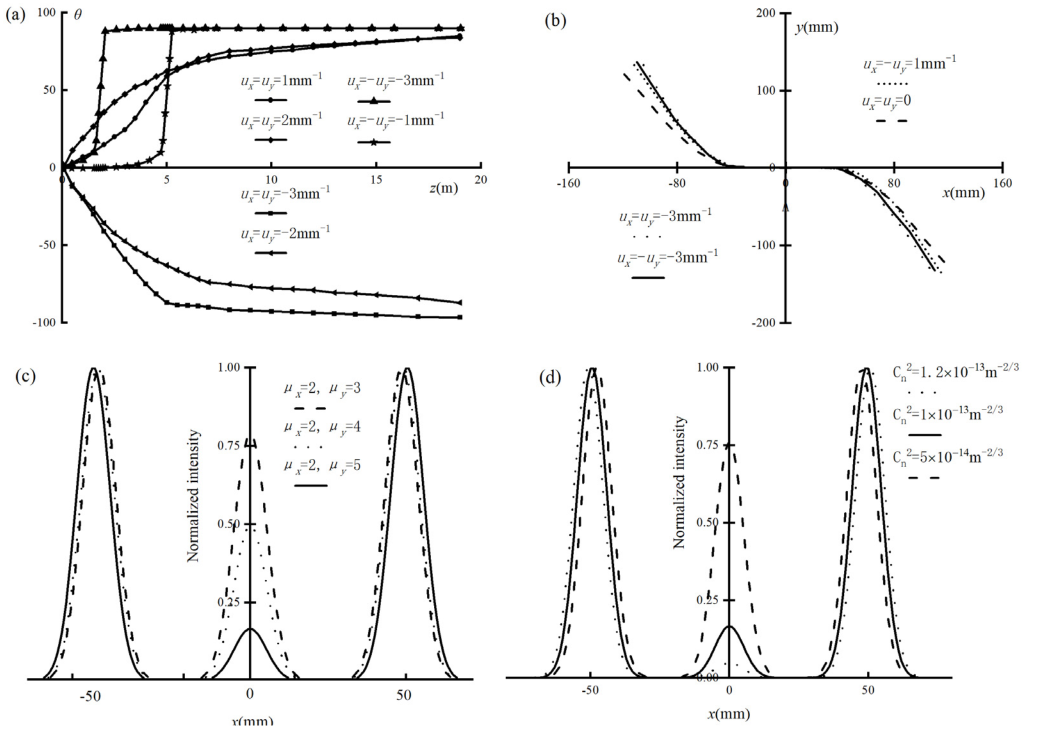

Fig. 4. Evolution of the EM TGSMA beam in conditions of different turbulence and twisted strength. Beam parameters are same as those in Fig. 2, except for twisted strengths $u_x = u_y = 1$ mm^{-1}; (c) $C_n^2 = 10^{-14}$ m$^{-2/3}$, and (d) $\mu_x = 2$, $\mu_y = 5$.

tating behavior of the array beams relies on the choice of the twisted strengths on propagation. The larger value of twist strengths leads to more obvious rotation of the EM TGSMA beam. When the sign of twisted strength u_x along x-direction is contrary to that of twisted strength u_y along y-direction, the rotation angle increases sharply from 0° to 90°. It means in this case that the intensity profiles change straightly from a horizontal ellipse to a vertical ellipse. Figure 4(b) presents the trajectories of the side lobes in the transverse plane when the propagation distance increases from 15 to 30 m at different values of twisted strengths. One can find that the two side-lobes move in the opposite direction from the initial position along the parabolas-like curves when propagation distance increases. The larger the anisotropic factors μ_x and μ_y, the faster the two side-lobes move along the y-direction. Figure 4(c) describes the change of center -lobe of the array beams along the x-direction at different values of anisotropic factors, and Fig. 4(d) illustrates the change of center-lobe of the array beams along the x-direction in different turbulent structure parameters. When the anisotropic factors μ_x and μ_y (as shown in Fig. 4(c)) or the turbulent structure constant C_n^2 (as shown in Fig. 4(d)) become larger, it can be seen from these figures that the spatial power spectrum intensity of atmospheric turbulence increases, resulting in a decrease of the central lobe, which also implies an increase of the two side-lobes.

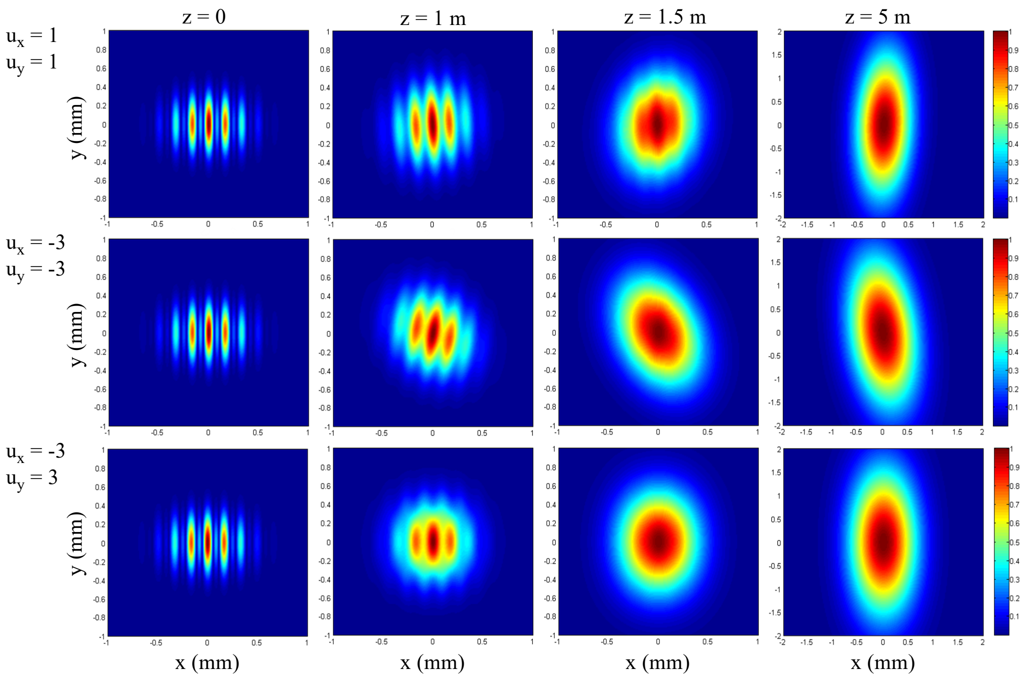

Fig. 5. Variation of modulus of the DOC for the EM TGSMA beam at several propagation distances through anisotropic atmosphere turbulence for different values of twisted strengths with parameters as in Fig. 2.

Secondly, we turn our attention to the DOC of the EM TGSMA beam. Figure 5 presents variation of the modulus of the array beams with the same source parameters as in Fig. 2 through anisotropic atmosphere turbulence at different values of twisted strengths. One can find that the DOC of the beams array also rotates around its center upon propagation and a Gaussian profile degenerates gradually from initial lattice-like profile. The variation of rotation angle depends on twisted strengths u_x and u_y, which behaves similar to Fig. 2, except in the opposite direction rotation. Figure 6 shows variation of the DOC of the EM TGSMA beam in different anisotropic turbulent conditions. One can see that anisotropic turbulent parameters play an important role in behavior of DOC of the array beams. When the anisotropic factors μ_x and μ_y (as shown in Fig. 6(a)) or the turbulent structure constant C_n^2 (as shown in Fig. 6(b)) increase, it can all cause more obvious broadening of DOC of the array beams.

Finally, we discuss the polarization properties of the EM TGSMA beam. In Fig. 7, we show evolution of the DOP of the array beams in different anisotropic turbulent conditions. It can be found that in the near field, the DOP of the array beams transforms from a certain cross-like shape into two symmetrical shapes arranged side by side with certain rotation, and rotational behavior of DOP varies with twisted strengths. When propagation distance of the array beams exceeds 15 m, the influence of anisotropic turbulence on DOP becomes increasingly obvious and symmetry of DOP is destroyed,

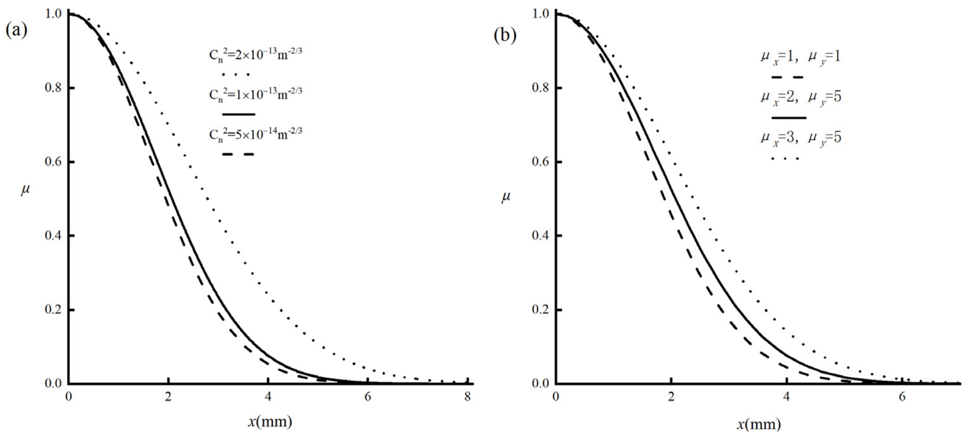

Fig. 6. Variation of DOC of the EM TGSMA beam in different anisotropic turbulent conditions, beams parameters are same as those in Fig. 2 except for twisted strength $u_x = u_y = 1\ \text{mm}^{-1}$. (a) $\mu_x = 2$, $\mu_y = 5$, and (b) $C_n^2 = 10^{-14}\ \text{m}^{-2/3}$.

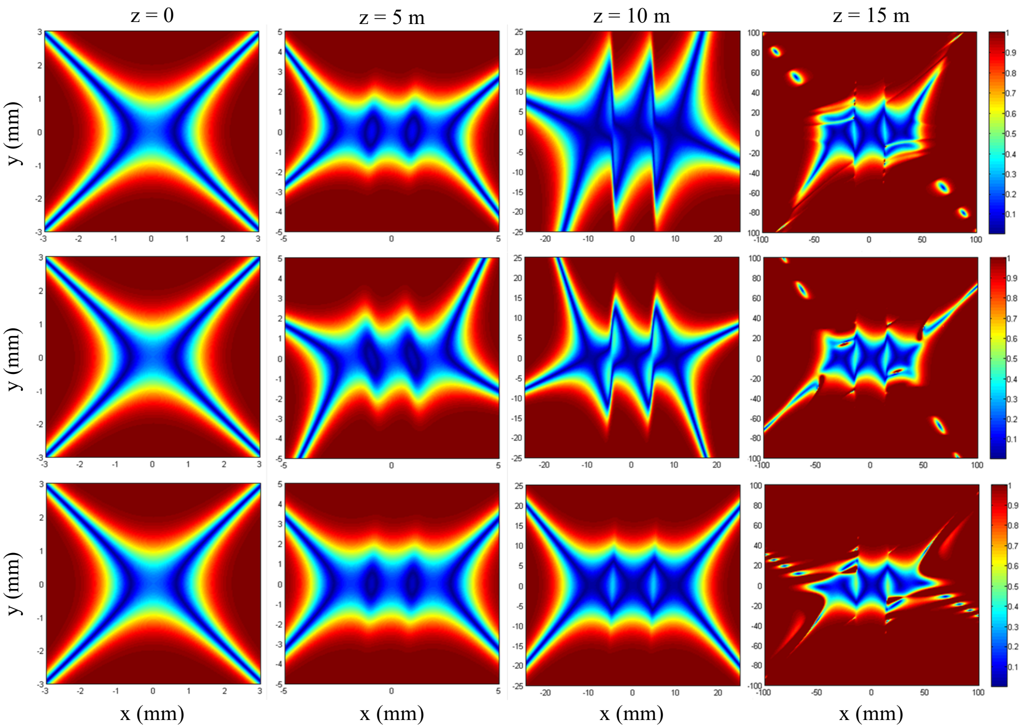

Fig. 7. Variation of DOP of the EM TGSMA beams through anisotropic atmosphere turbulence at different values of twisted strengths beam parameters are chosen: $\sigma_{1xx} = 0.5$ mm, $\sigma_{1yy} = 0.4$ mm, $\sigma_{2xx} = 0.4$ mm, $\sigma_{2yy} = 0.5$ mm, $\delta_{1xx} = \delta_{1yy} = 0.5$ mm, $\delta_{2xx} = \delta_{2yy} = 0.4$ mm, atmosphere turbulent parameters are set: $C_n^2 = 10^{-14}\ \text{m}^{-2/3}$, $\mu_x = 2$, and $\mu_y = 5$.

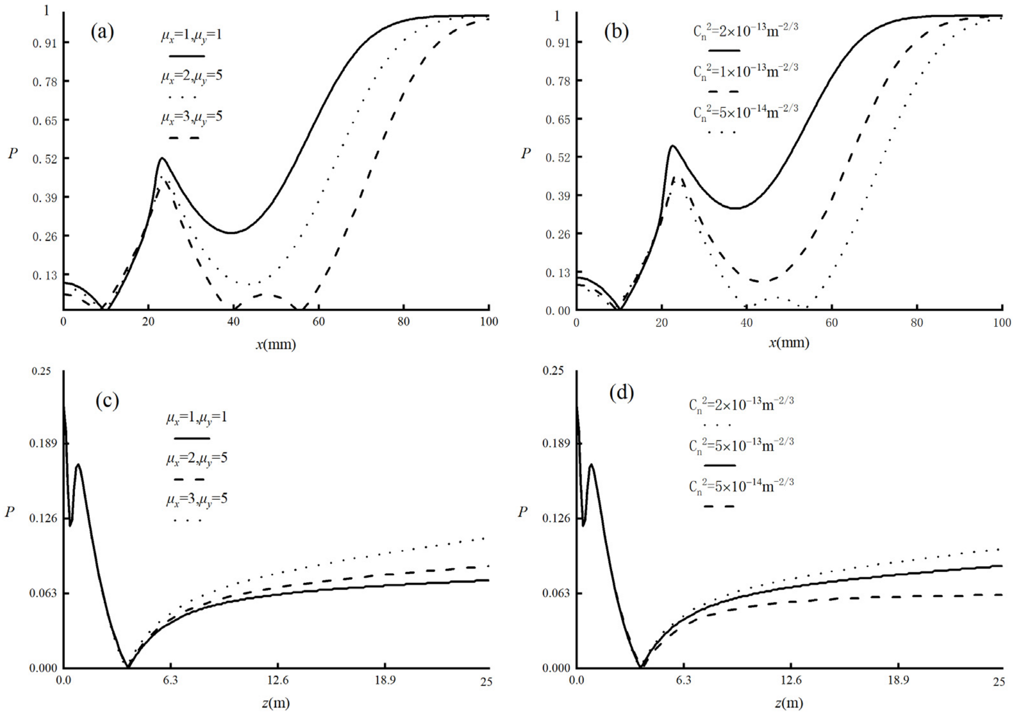

Fig. 8. Variation of polarization properties of the EM TGSMA beam through anisotropic atmosphere turbulence. Beam parameters are same as that in Fig. 7, except for twisted strengths $u_x = u_y = 1$. (a, b) Variation of DOP with the coordinates x at propagation distance $z = 25$ m. (c, d) The on-axis behaviors of DOP along propagation distance z. (a, c) $C_n^2 = 10^{-14}$ m$^{-2/3}$, and (b, d), $\mu_x = 2$, $\mu_y = 5$.

the value of DOP is closed to 1 in a large scale. Figure 8 shows the behavior of the DOP along the x-direction at a certain propagation distance and on-axis behavior of DOP along propagation distance z in anisotropic atmosphere turbulence, respectively. From Fig. 8(a)–(d), it can be seen that both the anisotropic factor and the turbulent structure constant increase, which has a significant effect on the DOP of the EM TGSMA beam. After a more district fluctuation, distribution of the DOP gradually approaches a certain value. Therefore, we can reach such conclusion that despite the anisotropic atmosphere turbulence has an important effect on the DOP of an EM TGSMA beam, with proper choices of source parameters and propagation distance, one can control, to some extent, the change in polarization properties of an EM TGSMA beam.

5. Conclusion

In this work, we have obtained an analytical expression for the cross-spectral density function of an EM TGSMA beams in anisotropic atmospheric turbulence based on the extended Huygens–Fresnel integral and investigated numerically the propagation properties of an EM TGSMA beam in detail. Particularly, we investigated the effects of twisted strengths and anisotropic atmospheric turbulence on the spectral density, DOP and DOC. The results indicate that the initial parameters of the array beams and anisotropic atmosphere turbulence play an important role on propagation properties of an EM TGSMA beam. For spectral intensity, the array beams go through rotation caused by twisted strength and mergence by anisotropic atmospheric turbulence. And for DOC of the array beams, the twisted strength always causes DOC of the array beams to rotate in an opposite direction compared with that of spectral density, and anisotropic atmospheric turbulence is responsible for the broadening of the DOC. Furthermore, apart from rotation, the distribution of DOP on the on-axis and transverse plane would tend to a certain value on propagation. The larger the value of the anisotropic factor and turbulent structure constant, the greater the final stable value of the DOP. Our results might be used for operation of communication, imaging, and sensing system.

Funding

This study was funded by the Science Foundation of Gansu Province in China (Grant number 21JR7RM188).

Conflict of interest

The authors declare that they have no conflict of interest.

References

[1] SIMON R., MUKUNDA N., *Twisted Gaussian Schell-model beams*, Journal of the Optical Society of America A **10**(1), 1993, pp. 95–109, DOI: 10.1364/JOSAA.10.000095.

[2] SERNA J., MOVILLA J.M., *Orbital angular momentum of partially coherent beams*, Optics Letters **26**(7), 2001, pp. 405–407, DOI: 10.1364/OL.26.000405.

[3] ZHAO C., CAI Y., KOROTKOVA O., *Radiation force of scalar and electromagnetic twisted Gaussian Schell-model beams*, Optics Express **17**(24), 2009, pp. 21472–21487, DOI: 10.1364/OE.17.021472.

[4] WANG F., CAI Y., *Second-order statistics of a twisted Gaussian Schell-model beam in turbulent atmosphere*, Optics Express **18**(24), 2010, pp. 24661–24672, DOI: 10.1364/OE.18.024661.

[5] ZHANG L., CAI Y., *Evolution properties of a twisted Gaussian Schell-model beams in a uniaxial crystal*, Journal of Modern Optics **58**(14), 2011, pp. 1224–1232, DOI: 10.1080/09500340.2011.599503.

[6] LIU L., HUANG Y., CHEN Y., GUO L., CAI Y., *Orbital angular moment of an electromagnetic Gaussan Schell-model beams with a twist phase*, Optics Express **23**(23), 2015, pp. 30283–30296, DOI: 10.1364/OE.23.030283.

[7] FRIBERG A.T., TERVONEN E., TURUNEN J., *Interpretation and experimental demonstration of twisted Gaussian Schell-model beams*, Journal of the Optical Society of America A **11**(6), 1994, pp. 1818–1826, DOI: 10.1364/JOSAA.11.001818.

[8] GORI F., SANTARSIERO M., *Devising genuine twisted cross-spectral densities*, Optics Letters **43**(3), 2018, pp. 595–598, DOI: 10.1364/OL.43.000595.

[9] BORGHI R., GORI F., GUATTARI G., SANTARSIERO M., *Twisted Schell-model beamss with axial symmetry*, Optics Letters **40**(19), 2015, pp. 4504–4507, DOI: 10.1364/OL.40.004504.

[10] BORGHI R., *Twisting partially coherent light*, Optics Letters **43**(8), 2018, pp. 1627–1630, DOI: 10.1364/OL.43.001627.

[11] MEI Z., KOROTKOVA O., *Random sources for rotating spectral densities*, Optics Letters **42**(2), 2017, pp. 255–258, DOI: 10.1364/OL.42.000255.

[12] YU H., SHE W., *Rotation dynamics of particles trapped in a rotating beams*, Journal of the Optical Society of America A **32**(1), 2015, pp. 90–100, DOI: 10.1364/JOSAA.32.000090.

[13] Paterson L., MacDonald M.P., Arlt J., Sibbett W., Bryant P.E., Dholakia K., *Controlled rotation of optically trapped microscopic particles*, Science **292**(5518), 2001, pp. 912–914, DOI: 10.1126/science.1058591.
[14] Wang F., Cai Y., Eyyuboğlu H.T., Baykal Y., *Twist phase-induced reduction in scintillation of a partially coherent beams in turbulent atmosphere*, Optics Letters **37**(2), 2012, pp. 184–186, DOI: 10.1364/OL.37.000184.
[15] Zilberman A., Golbraikh E., Kopeika N.S., VirtserA., Kupershmidt I., Shtemler Y., *Lidar study of aerosol turbulence characteristics in the troposphere: Kolmogorov and non-Kolmogorov turbulence*, Atmospheric Research **88**(1), 2008, pp. 66–77, DOI: 10.1016/j.atmosres.2007.10.003.
[16] Johnson L.J., Green R.J., Leeson M.S., *Underwater optical wireless communications: depth-dependent beams refraction*, Applied Optics **53**(31), 2014, pp. 7273–7277, DOI: 10.1364/AO.53.007273.
[17] Hou W., Jarosz E., Woods S., Goode W., Weidemann A., *Impacts of underwater turbulence on acoustical and optical signals and their linkage*, Optics Express **21**(4), 2013, pp. 4367–4375, DOI: 10.1364/OE.21.004367.
[18] Shchepakina E., Farwell N., Korotkova O., *Spectral changes in stochastic light beams propagating in turbulent ocean*, Applied Physics B **105**, 2011, pp. 415–420, DOI: 10.1007/s00340-011-4626-9.
[19] Farwell N., Korotkova O., *Intensity and coherence properties of light in oceanic turbulence*, Optics Communications **285**(6), 2012, pp. 872–875, DOI: 10.1016/j.optcom.2011.10.020.
[20] Fu W., Zhang H., *Propagation properties of partially coherent radially polarized doughnut beams in turbulent ocean*, Optics Communications **304**, 2013, pp. 11–18, DOI: 10.1016/j.optcom.2013.03.029.
[21] Korotkova O., Farwell N., Shchepakina E., *Light scintillation in oceanic turbulence*, Waves in Random and Complex Media **22**(2), 2012, pp. 260–266, DOI: 10.1080/17455030.2012.656731.
[22] Ata Y., Baykal Y., *Scintillation of optical plane and spherical waves in underwater turbulence*, Journal of the Optical Society of America A **31**(7), 2014, pp. 1552–1556, DOI: 10.1364/JOSAA.31.001552.
[23] Baykal Y., *BER of asymmetrical optical beams in oceanic and marine atmospheric media*, Optics Communications **393**, 2017, pp. 29–33, DOI: 10.1016/j.optcom.2017.02.023.
[24] Keskin A., Baykal Y., *Scintillation and BER analysis of cosine and cosine-hyperbolic-Gaussian beams in turbulent ocean*, Applied Optics **60**(24), 2021, pp. 7054–7063, DOI: 10.1364/AO.428840.
[25] Lu L., Ji X. L., Baykal Y., *Wave structure function and spatial coherence radius of plane and spherical waves propagating through oceanic turbulence*, Optics Express **22**(22), 2014, pp. 27112–27122, DOI: 10.1364/OE.22.027112.
[26] Fu W., Cao P., *Second-order statistics of a radially polarized partially coherent twisted beams in a uniaxial crystal*, Journal of the Optical Society of America A **34**(9), 2017, pp. 1703–1710, DOI: 10.1364/JOSAA.34.001703.
[27] Fu W., Zheng X., *Influence of anisotropic turbulence on the second-order statistics of a general -type partially coherent beam in the ocean*, Optics Communications **438**, 2019, pp. 46–53, DOI: 10.1016/j.optcom.2018.12.089.
[28] Cui L., Xue B., Zhou F., *Generalized anisotropic turbulence spectra and applications in the optical waves' propagation through anisotropic turbulence*, Optics Express **23**(23), 2015, pp. 30088–30103, DOI: 10.1364/OE.23.030088.
[29] Galperin B., Sukoriansky S., Dikovskaya. N., Read P.L., Yamazaki Y.H., Wordsworth R., *Anisotropic turbulence and zonal jets in rotating flows with a β-effect*, Nonlinear Processes in Geophysics **13**(1), 2006, pp. 83–98, DOI: 10.5194/npg-13-83-2006.
[30] Andrews L.C., Phillips R.L., Crabbs R., *Propagation of a Gaussian-beams wave in general anisotropic turbulence*, Proc. SPIE 9224, Laser Communication and Propagation through the Atmosphere and Oceans III, (3 October 2014), article no. 922402, DOI: 10.1117/12.2061892.
[31] Berger V., Gauthier-Lafaye O., Costard E., *Photonic band gaps and holography*, Journal of Applied Physics **82**(1), 1997, pp. 60–64, DOI: 10.1063/1.365849.
[32] Campbell M., Sharp D.N., Harrison M.T., Denning R.G., Turberfield A.J., *Fabrication of photonic crystals for the visible spectrum by holographic lithography*, Nature **404**, 2000, pp. 53–56, DOI: 10.1038/35003523.

[33] BLOCH I., *Ultracold quantum gases in optical lattices*, Nature Physics **1**, 2005, pp. 23–30, DOI: 10.1038/nphys138.
[34] MACDONALD M.P., SPALDING G.C., DHOLAKIA K., *Microfluidic sorting in an optical lattice*, Nature **426**, 2003, pp. 421–424, DOI: 10.1038/nature02144.
[35] ZHENG S., HUANG J., JI X., CHENG K., WANG T., *Rotating anisotropic Gaussian Schell-model array beams*, Optics Communications **484**, 2021, article no. 126684, DOI: 10.1016/j.optcom.2020.126684.
[36] WAN L., ZHAO D., *Twisted Gaussian Schell-model array beams*, Optics Letters **43**(15), 2018, pp. 3554–3557, DOI: 10.1364/OL.43.003554.
[37] ZHOU Y., ZHAO D., *Statistical properties of electromagnetic twisted Gaussian Schell-model array beams during propagation*, Optics Express **27**(14), 2019, pp. 19624–19632, DOI: 10.1364/OE.27.019624.
[38] TOSELLI I., AGRAWAL B., RESTAINO S., *Light propagation through anisotropic turbulence*, Journal of the Optical Society of America A **28**(3), 2011, pp. 483–488, DOI: 10.1364/JOSAA.28.000483.
[39] WOLF E., *Unified theory of coherence and polarization of random electromagnetic beams*, Physics Letters A **312**(5–6), 2003, pp. 263–267, DOI: 10.1016/S0375-9601(03)00684-4.

Received March 6, 2022
in revised form May 3, 2022